Electronic Supplementary Information (ESI)

A chlorinated polythiophene-based polymer as a dopant-free hole transport material in perovskite solar cells

Kakaraparthi Kranthiraja[a], Ryosuke Nishikubo[a,b], Akinori Saeki[a,b*]

[a]Department of Applied Chemistry, Graduate School of Engineering, Osaka University, 2-1 Yamadaoka, Suita, Osaka 565-0871, Japan.

[b]Innovative Catalysis Science Division, Institute for Open and Transdisciplinary Research Initiatives (ICS-OTRI), Osaka University, 1-1 Yamadaoka, Suita, Osaka 565-0871, Japan.

*E-mail: saeki@chem.eng.osaka-u.ac.jp

Experimental.

Materials. 3-chlorothiophene was purchased from Matrix scientific (USA). NBS, PbI_2, MAI and FAI were purchased from TCI (Japan), PTAA**,** chlorobenzene, trimethyl tin chloride, and *n*-BuLi were purchased from Sigma Aldrich. Tetrahydrofuran, DMF and DMSO were purchased from the Wako (Japan).

Synthesis of polymer.

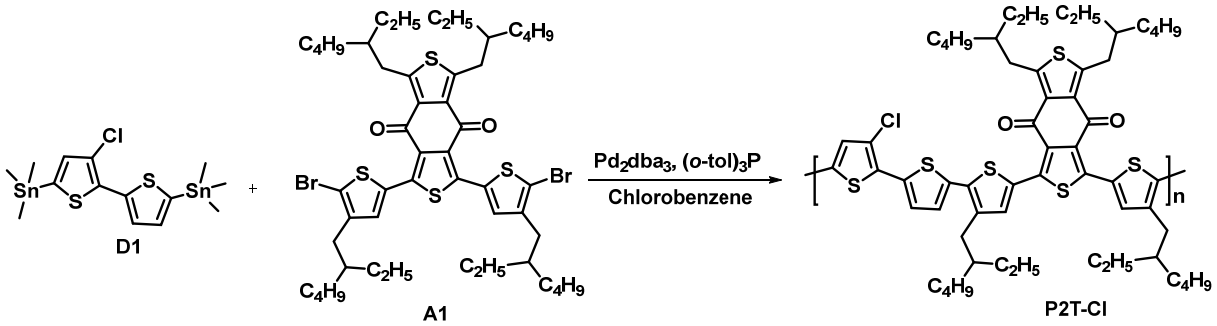

Scheme 1. Synthetic route for new polymer P2T-Cl.

The key monomers D1 and A1, P2T (polymer) were synthesized according to the reported procedures[S2-S4]. P2T-Cl was characterized by ^{1}H NMR, and M_n and M_{wt} of the polymers were estimated by gel permeation chromatography.

Synthesis of poly(1-(3''-chloro-3-(2-ethylhexyl)-[2,2':5',2''-terthiophen]-5-yl)-alt-5,7-bis(2-ethylhexyl)-3-(4-(2-ethylhexyl)thiophen-2-yl)-4H,8H-benzo[1,2-c:4,5-c']dithiophene-4,8-dione) (P2T-Cl). The monomers D1 (0.08 g, 0.15 mmol), and A1 (0.15 g, 0.15 mmol), were dissolved in anhydrous CB (5 mL) and purged with nitrogen for 15 min before the addition of Pd_2dba_3 (2.5 mg), (*o*-tol)$_3$P (5 mg) and continued the purging for 15 min, heated to 120 °C for 30 minutes. After completion of the reaction, cooled the reaction mixture and precipitated into methanol. Then Soxhlet extraction was carried out with methanol, hexane, acetone and chloroform, the chloroform fraction was evaporated and precipitated from methanol to get *P2T-Cl (yield=70 %)*. GPC: M_n = 16.4 kg mol^{-1}; PDI = 1.5. ^{1}H NMR (400 MHz, $CDCl_3$): 7.51-7.60 (br, 2H), 7.01-7.10 (br, 3H), 3.30 (br, 4H), 2.75 (br, 4H), 1.77 (br, 4H), 1.23-1.50 (br, 32H), 0.93 (br, 12H).

General Measurement. ^{1}H NMR (400 MHz) spectra were measured on a JEOL JNM-ECZS400 spectrometer. Steady-state photo absorption spectra were recorded using a JASCO V-570 UV−vis spectrophotometer. The molecular weight and polydispersity index (PDI) of polymers were measured using the size exclusion chromatography (gel permeation chromatography: GPC, a Shimadzu Corp. LC20AT/CBM-20A/CTO-20A/ SPD-M20A) with polystyrene standards in hot chloroform (40 °C) as an eluent. Photoelectron yield spectroscopy (PYS) of the polymer films on indium-tin-oxide (ITO) glass was performed using Bunko Keiki BIP-KV202GD. 2D-GIXRD experiments were performed on the beam line BL46XU at the SPring-8 (12.39 keV, λ =1 Å X-ray). The 2D-GIXRD patterns were monitored with a 2D image detector (Pilatus 300 K). AFM was

performed using a Bruker Innova AFM microscope. Thicknesses of the polymer films were measured using a Bruker Dektak XT surface profiler. CA of films were measured using an Asumi Giken CAME1 with water. TRMC was performed for the polymer:perovskite films prepared on a quartz substrate.

Device Fabrication.

A FTO layer on a glass substrate was etched with 6 mol dm^{-3} HCl and Zn using masking tape. After cleaning with detergent, acetone, isopropyl alcohol, and deionized water, a compact TiO_2 (c-TiO_2) layer was deposited onto the FTO/glass by spray pyrolysis using a solution of titanium diisopropoxide bis(acetylacetonate) (Tokyo Chemical Industry Co. Ltd, TCI) in ethanol (1 : 14 v/v) at 450 ℃. A 200 nm-thick mesoporous TiO_2 (mpTiO_2) layer (average particle size: 30 nm, anatase) was deposited onto the compact TiO_2 layer by spin-coating (slope 3 s, 5000 rpm for 15 s, slope 2 s) of a diluted TiO_2 paste (PST–30NR-D, GreatCell Solar Ltd.) in ethanol (paste : ethanol = 1 : 7 w/w), followed by sintering at 500 ℃ for 20 min. For perovskite deposition, a 1.4 M *N*,*N* -dimethylformamide (DMF, super dehydrated, Wako) : dimethyl sulfoxide (DMSO, super dehydrated, Wako) = 4 : 1 (v/v%) solution of FAI ($(NH_2)_2CHI$), PbI_2, MABr (CH_3NH_3Br), and $PbBr_2$ with a 0.87 : 0.13 stoichiometry (the amount of FAI was reduced to FAI/PbI_2 = 0.95) was prepared in an N_2-filled glovebox. These perovskite precursors of solar cell grade were purchased from Tokyo Chemical Inc. (TCI) and used as received. Subsequently, a precursor layer was formed by spin-coating the solution (slope 1 s, 1000 rpm for 10 s, slope of 4 s, 4500 rpm for 30 s, slope of 2 s). After 35 s, anti-solvent treatment (chlorobenzene, anhydrous 99.8%, Sigma-Aldrich) was applied by slowly dropping 180 mL onto the rotating substrate. The perovskite film was annealed at 100 ℃ for 30 min. For the deposition of SbSI:Sb_2S_3 film on mp-TiO_2, a DMSO solution of SbI_3 and Sb-ethyl xanthate was spin-coated and annealed as described in our report.[S1] A 25-30 nm-thick of P2T or P2TCl were deposited by spin-coating of 10 mg / mL chlorobenzene (Sigma-Aldrich, anhydrous, 99.8%) at 3000 rpm. A 25 nm-thick of PTAA (Aldrich) was deposited by spin-coating of 10 mg m L^{-1} toluene (Wako, anhydrous, 99.5%) without dopants. Subsequently, a top electrode (80 nm Au) was deposited through a shadow mask by thermal evaporation in a vacuum chamber. The solar cell characteristics were measured using an ADCMT Corp., 6241A source meter unit under air mass 1.5 G solar illumination at 100 mW cm^{-2} (1 sun, monitored by a calibrated standard cell, Bunko Keiki SM250KD) from a 300 W solar simulator (SAN-EI Corp., XES301S). The external quantum efficiency (EQE) spectra were recorded using a Bunko Keiki model BS-520BK equipped with a Keithley model 2401 source meter. The monochromatic light power for EQE measurements was calibrated by a silicon photovoltaic cell of a Bunko Keiki model S1337-1010BQ. Stability test of PSCs was performed by keeping the devices in an environmental test chamber (ESPEC Corp. SH-222) at 30℃ and relative humidity of 60% in darkness.

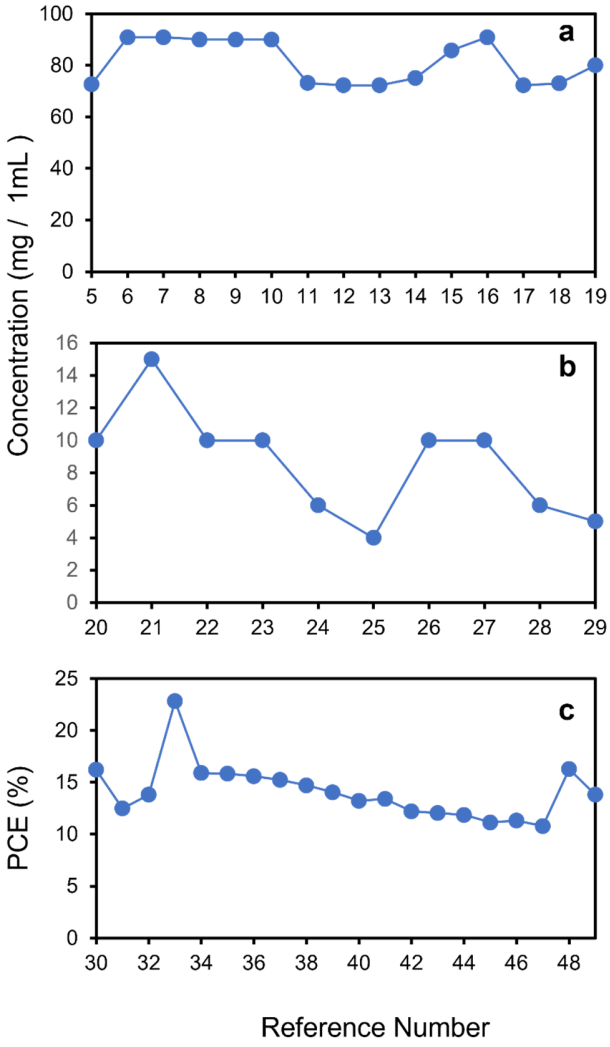

Figure S1 (a-c). Small molecule HTM (Spiro-OMeTAD) concentration from 15 different reference papers, polymer HTM (PTAA and others) concentration from 10 different reference papers and PCE summary of P3HT based PSCs from 20 different reference papers.

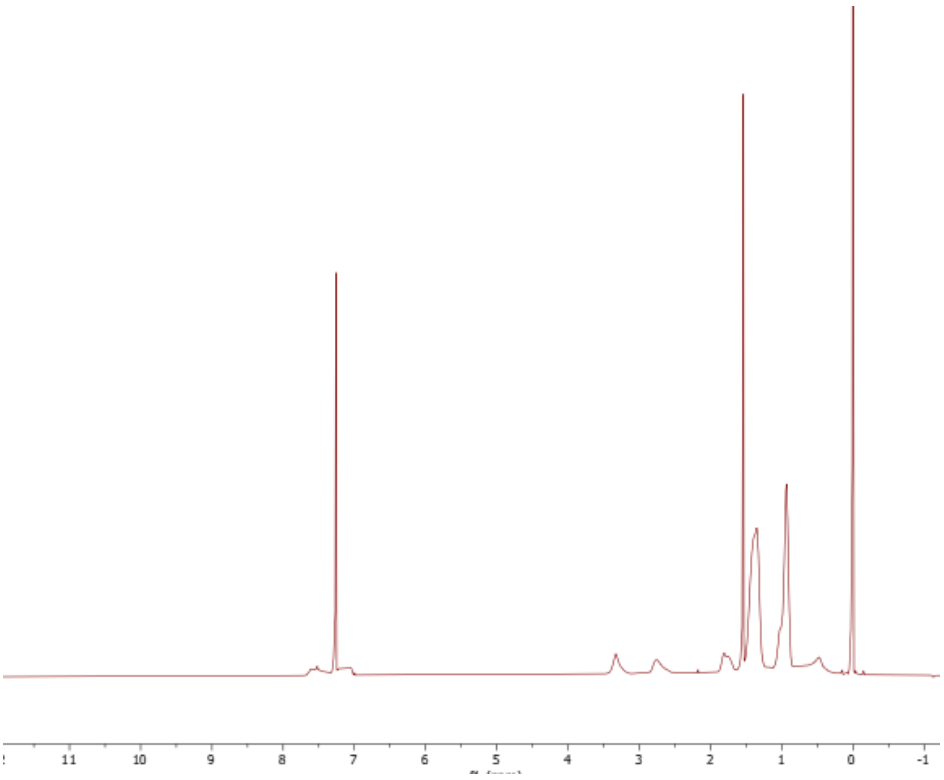

Figure S2. ^{1}H NMR of P2T-Cl.

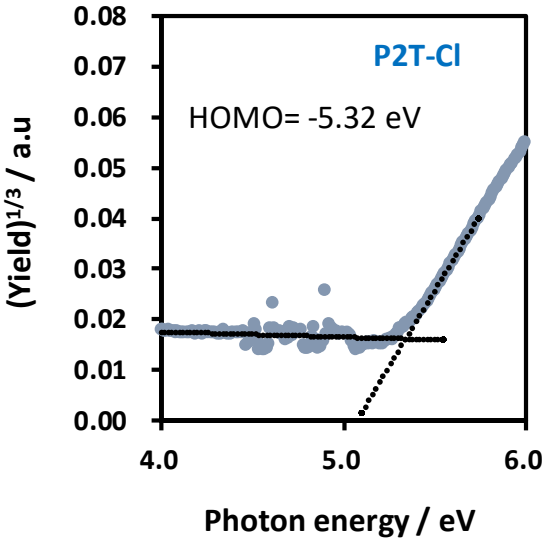

Figures S3. PY spectrum to evaluate HOMO energy level of P2T-Cl.

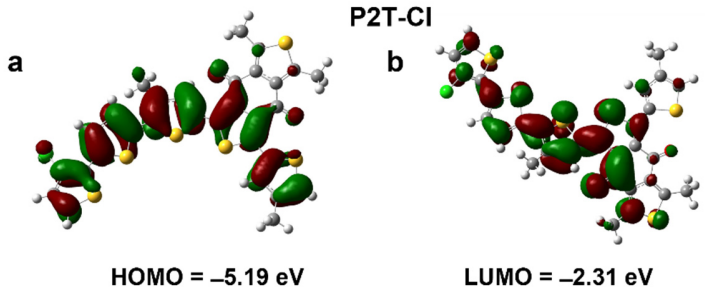

Figure S4. (a, b) DFT calculated HOMO and LUMO of repeating unit (P2T-Cl). The alkyl chains were replaced by methyl for simplicity.

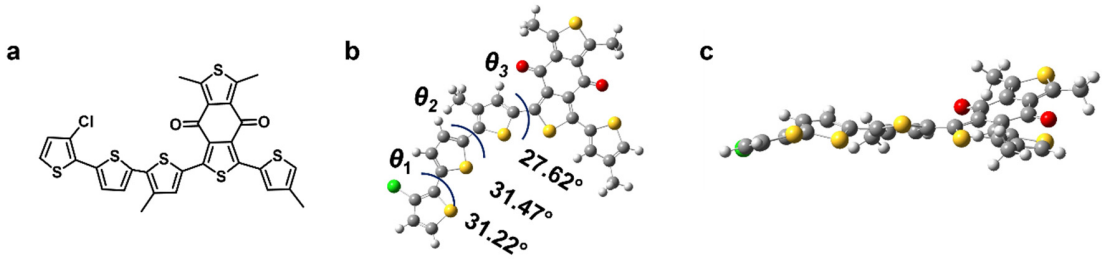

Figure S5. (a-c) Chemical structure, front-view, and side view of repeating unit of P2T-Cl. The alkyl chains were replaced by methyl for simplicity.

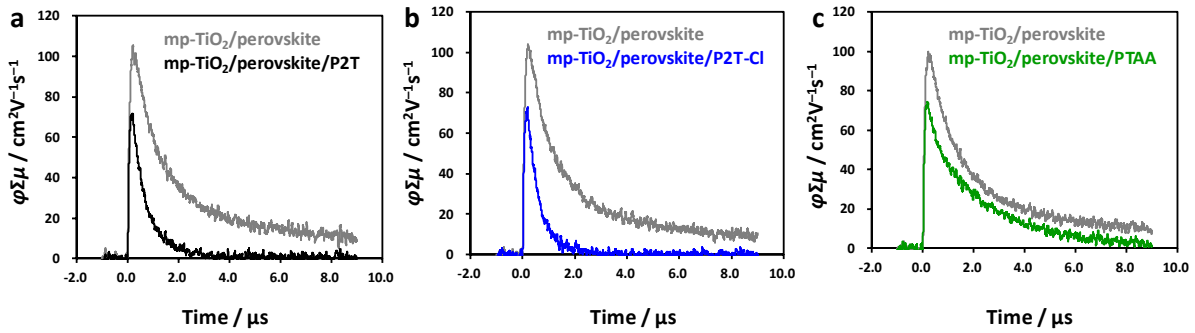

Figure S6. (a). TRMC transients ($\varphi\Sigma\mu$) of mp-TiO_2:perovskite and mp-TiO_2: perovskite:P2T; (b) mp-TiO_2:perovskite and mp-TiO_2:perovskite:P2T-Cl; (c) mp-TiO_2:perovskite and mp-TiO_2:perovskite:PTAA.

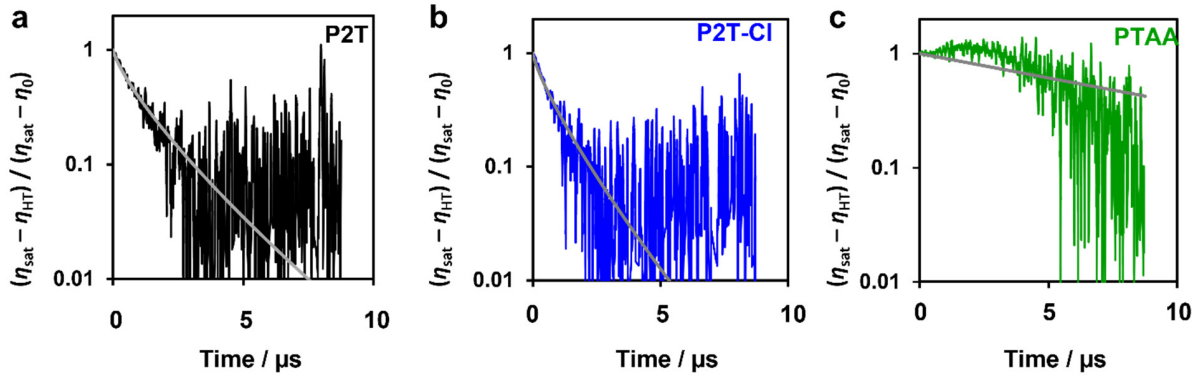

Figure S7. Semilogarithmic plot of normalized η_{HT} given by $(\eta_{sat} - \eta_{HT}) / (\eta_{sat} - \eta_0)$ vs time of P2T, P2T-Cl and PTAA. η_0 and η_{sat} represents the hole transfer yield at the pulse end and the deay end, respectively. The gray solid lines are fitted line using a streched exponential function.

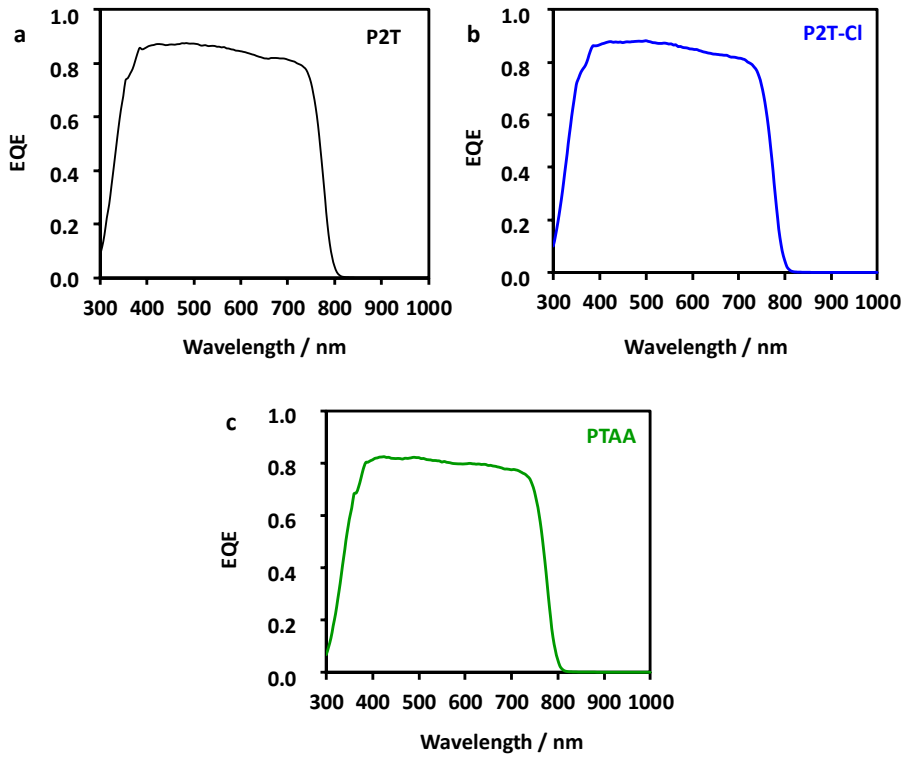

Figure S8. (a-c) EQE spectra of P2T, P2T-Cl, and PTAA based PSCs.

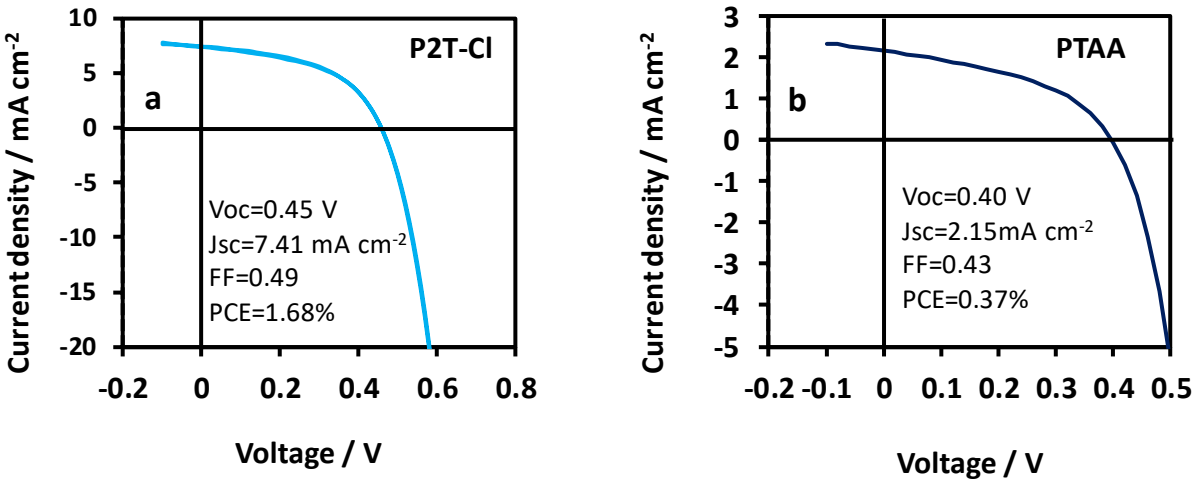

Figure S9 . (a) *J-V* curve of P2T-Cl based SbSI:Sb_2S_3 solar cell (b) *J-V* curve of PTAA (undoped) based SbSI: Sb_2S_3 solar cell.

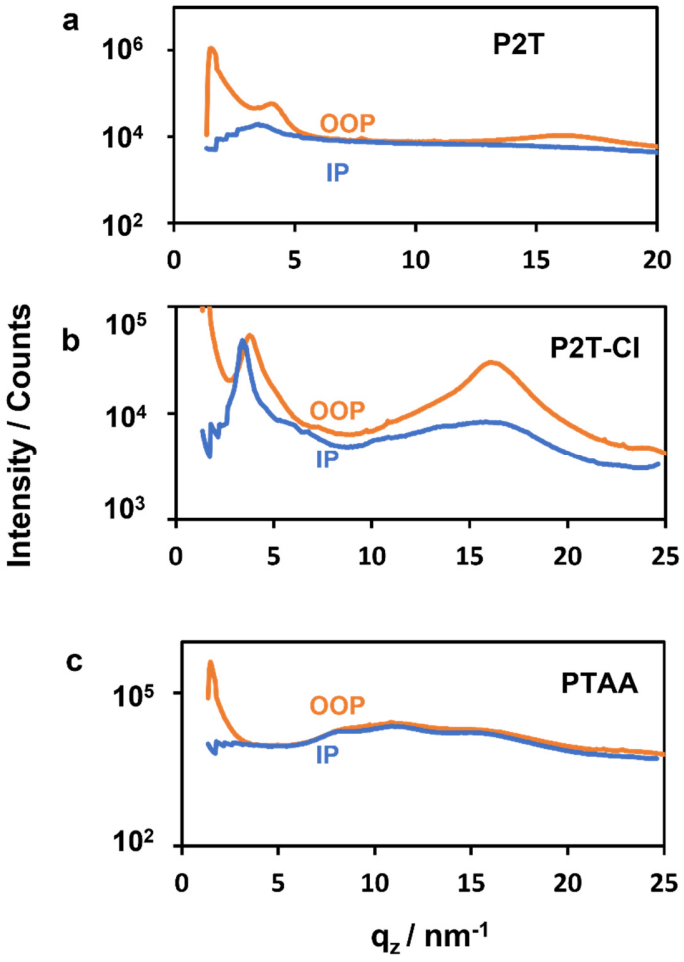

Figure S10. 2D-GIXRD diffraction line cuts (a-c) P2T (from refernce S4); P2T-Cl and PTAA.

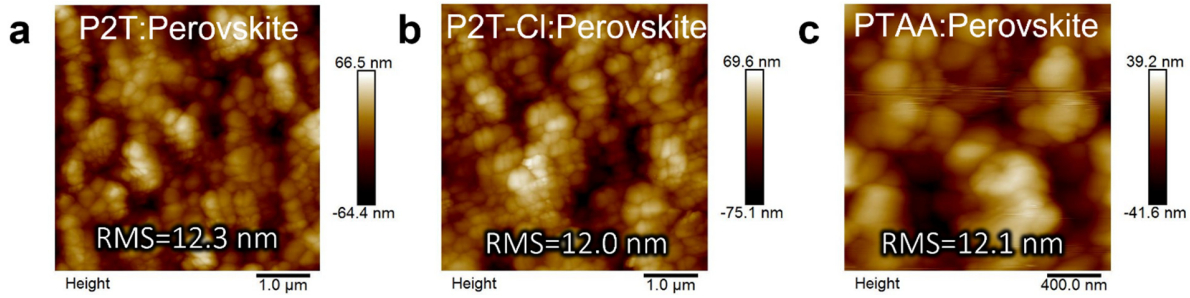

Figure S11. (a-c) AFM images of P2T, P2T-Cl and PTAA on perovskite surface.

Table 1. Cost calculation of P2T-Cl (Cost is in USD, chemicals were purchased from Sigma, TCI, Matrix, BLD, Kanto Japan etc

Chemical	Reagent cost/ $	Solvent volume / mL	Solvent cost / $	Reagent+solvent cost / $	Product cost / 1g
3-Chlorothiophene / 1 g	0.86			0.86	
NBS / 1.5 g	2.25			2.25	
$CHCl_3$		20 mL	0.05	0.05	
CH_3COOH		20 mL	1.56	1.56	
CH_2Cl_2		100 mL	0.26	0.26	
Hexane		500 mL	0.79	0.79	
Total cost				5.77	
Product step 1 (Yield=78%, 1.3g)					4.43
2-tributylstannyl thiophene (2.07 g)	9.81			9.81	
Pd $(PPh_3)_4$ (0.025 g)				0.54	
Toluene (10 mL)				0.52	
Hexane (1 L)				1.58	
CH_2Cl_2 (100 mL)				0.26	
Total cost				12.71	
Product step 2 (yield = 75%, 0.82 g)					15.5
n-BuLi (4.98 mL)	3.48				
Trimethyl tin chloride	7.56				
THF (20 mL)				0.54	
CH_2Cl_2 (100 mL)				0.26	
Total Cost				11.84	
Product step 3 (yield = 90%, 2.4g)					4.93
3,4-thiophene dicarboxylic acid (1g)	5.6				
Bromine (0.75 mL)				0.04	
Acetic acid (10 mL)				0.78	
Total cost				6.42	
Product step 4 (yield = 81%, 1.55g)					4.0
Thiophene (1g)	0.09				
2-ethylhexyl bromide (4.82 g)	1.47				
n-BuLi (10.5 mL)	7.35				
THF (25 mL)				0.67	
Hexane (1 L)				1.58	
Total cost				11.16	

Product Step 5 (yield = 68%; 2.5 g)				4.46
$AlCl_3$ (2 g)	0.22			
Oxalyl chloride (2 mL)	1.42			
Product 4 (1 g)				
Product 5 (1.25 g)				
CH_2Cl_2 (200 mL)			0.52	
Hexane (1 L)			1.58	
Total cost			3.74	
Product Step 6 (yield = 68%, 1.25 g)				2.99
3-ethylhexyl thiophene (1g)	21			
n-BuLi (2.03 mL)		1.42		
THF (20 mL)		0.54		
Tibutyltin chloride (1.65)		0.66		
CH_2Cl_2 (100 mL)		0.26		
Total cost			23.88	
Product 7 (yield=80%; 2 g)				11.94
Product 7 (1g)				
Product 6 (1g)				
$Pd(PPh_3)_4$ (25 mg)		0.54		
Toluene (20 mL)		1.04		
Hexane (1 L)		1.58		
Dichloromethane (200 mL)		0.52		
Total cost		3.68		
Product 8 (yield =72%; 1g)				3.68
Product 8				
NBS (0.54)		0.12		
THF (20 mL)		0.54		
Hexane (1 L)		1.58		
CH_2Cl_2 (500 mL)		1.3		
Total cost		3.54		
Product 9 (yield=63%; 0.75 g)				4.72
Product 3 (0.1 g)			2.48	
Product 9 (0.2 g)			5.55	
Chlorobenzene (6 mL)			0.96	
Pd_2dba_3 (10 mg)	0.79			
$(o\text{-}tol)_3P$ (20 mg)	0.03			
Methanol (200 mL)			0.31	
Acetone (200 mL)			0.50	
Hexane (200 mL)			0.79	
Chloroform (200 mL)			0.75	
Total cost			12.66	

Product 10 (yield=70%; 0.145 g)	99.97
Silica gel for total synthesis	75
1 gram of P2T-Cl	231
Regio regular-P3HT (100 mg) / TCI	255
PTAA/Sigma	421

Table S2. Orientations and crystal sizes evaluated by 2D-GIXRD.

Polymer	I_{IP}/I_{OOP} [a]	d_{IL} / Å [b]	L_{100} / nm [b]	$d_{\pi\text{-}\pi}$/ Å [c]	L_{010} / nm [c]
P2T [S4]	0.73	15.3	7.3	3.84	2.4
P2T-Cl	1.02	16.7	8.6	3.90	2.9
PTAA	N/A	N/A	N/A	N/A	N/A

[a] The portion of polymer orientation in crystallites evaluated from relative intensities of the (100) diffraction in the out-of-plane (I_{OOP}) and in-plane (I_{IP}) direction. The high I_{IP}/I_{OOP} represents more face-on orientation. [b] Interlamellar distance (d_{IL}) and crystal size (L_{100}) evaluated from the out-of-plane (100) diffraction. [c] π-π stacking distance ($d_{\pi\text{-}\pi}$) and crystal size (L_{010}) evaluated from the out-of-plane (010) diffraction. No diffraction peak was observed for PTAA.

REFERENCES

(S1) R. Nishikubo, H. Kanda, I. García-Benito, A. Molina-Ontoria, G. Pozzi, A.M.Asiri, M. K. Nazeeruddin,; Saeki, A. *Chem. Mater.* 2020, **32**, 6416–6424.

(S2) H. Chen, Z. Hu, H. Wang, L. Liu, P. Chao, J. Qu, W. Chen, A. Liu, F. He, *Joule*, 2018, **2**, 1623-1634.

(S3) U. K. Aryal, S. S. Reddy, K. Kranthiraja, J. Kim, W. Cho, M. Song, S.-H. Jin, *ACS Appl. Energy Mater.* 2019, **2**, 4159–4166.

(S4) K. Kranthiraja, A. Saeki, *ACS Appl. Polym. Mater.* 2021, **3**, 2759−2767.

(S5) B. Zhang, J. Oh, Z. Sun, Y. Cho, S. Jeong, X. Chen, K. Sun, F. Li, C. Yang, S. Chen, *ACS Energy Lett.* 2023, **8**, 1848–1856

(S6) A.-F. Castro-Méndez, J. P. Wooding, S. Fairach, C. A. R. Perini, E. K. McGuinness, J. N. Vagott, R. Li, S. Kim, V. Brahmatewari, N. Dentice, M. D. Losego, J.-P. Correa-Baena, *ACS Energy Lett.* 2023, **8**, 844–852

(S7) T. Yang, W. Zhao, Y. Yang, W. Huang, K. Zhao, S. Liu, *Adv. Mater.* 2023, DOI: 10.1002/adma.202211006

(S8) K. Liu, Y. Luo, Y. Jin, T. Liu, Y. Liang, L. Yang, P. Song, Z. Liu, C. Tian, L. Xie, Z. Wei, *Nat. Commun.* 2022, **13**, 4891.

(S9) S. Bentov, P. Zaslansky, A. Al-Sawalmih, A. Masic, P. Fratzl, A. Sagi, A. Berman, B. Aichmayer, *Nat Commun* 2013, **14**, 839.

(S10) M. Jeong, I. W. Choi, K. Yim, S. Jeong, M. Kim, S. J. Choi, Y. Cho, J.-H. An, H.-B. Kim, Y. Jo, S.-H. Kang, J.-H. Bae, C.-W. Lee , D. S. Kim , C. Yang, *Nat. Photon.* 2022, **16**, 119-125.

(S11) N. Y. Nia, F. Matteocci, L. Cina, A. D. Carlo, *ChemSusChem* 2017, **10**, 3854-3860.

(S12) G. -W. Kim, G. Kang, J. Kim, G.-Y. Lee, H. I. Kim, L. Pyeon, J. Leeb, T. Park, *Energy Environ. Sci.,* 2016, **9**, 2326-2333.

(S13) J. Lee, M. M. Byranvand, G. Kang, S. Y. Son, S. Song, G.-W. Kim, T. Park, *J. Am. Chem. Soc.* 2017, **139**, 12175−12181

(S14) J. Xia, P. Luizys, M. Daskeviciene, C. Xiao, K. Kantminiene, V. Jankauskas, K. Rakstys, G. Kreiza, X.-X. Gao, H. Kanda, K. G. Brooks, I. R. Alwani, Q. U. Ain, J. Zou, G. Shao, R. Hu, Z. Qiu, A. Slonopas, A. M. Asiri, Y. Zhang, P. J. Dyson, V. Getautis, M. K. Nazeeruddin, *Adv. Mater*. 2023, DOI: 10.1002/adma.202300720.

(S15) Z. Yao, F. Zhang, L. He, X. Bi, Y. Guo, Y. Guo, L. Wang, X. Wan, Y. Chen, L. Sun, *Angew. Chem., Int. Ed.* 2022, 61, e202114341.

(S16). S. D. -Geguziene, Y. Zhang, K. Rakstys, C. Xiao, J. Xia, Z. Qiu, M. Daskeviciene, T. Paskevicius, V. Jankauskas, A. M. Asiri, V. Getautis, M. K. Nazeeruddin, *Adv. Funct. Mater.*2023, **33**, 2208317.

(S17) E. Tanaka, G. M. Kim, M. R. Maciejczyk, A. Ishii, G. S. Nichol, T. Miyasaka, N. Robertson, *J. Mater. Chem. C* 2023 DOI: 10.1039/D3TC00119A.

(S18) L. Xu, P. Huang, J. Zhang, X. Jia, Z. Ma, Y. Sun, Y. Zhou, N.-Y. Yuan, J.-N. Ding, *J. Phys. Chem. C* 2018, **122**, 26337−26343.

(S19) C. Kou, S. Feng, H. Li, W. Li, D. Li, Q. Meng, Z. Bo, *ACS Appl. Mater. Interfaces* 2017, **9**, 43855–43860.

(S20) K. Kranthiraja, K. Gunasekar, H. Kim, A.-N. Cho, N.-G. Park, S. Kim, B. J. Kim, R. Nishikubo, A. Saeki, M. Song, S.-H. Jin, *Adv. Mater.* 2017, **29**, 1700183.

(S21) G.-W. Kim, J. Lee, G. Kang, T. Kim, T. Park, *Adv. Energy Mater.*2018, **8**, 1701935.

(S22) J. M. Marin-Beloqui, J. P. Hernándeza, E. Palomares, *Chem. Commun.,* 2014, **50**, 14566-14569.
(S23) J.-W. Lee, S. Park, M. J. Ko, H. J. Son, N.-G. Park, *Chem.Phys.Chem* 2014, **15**, 2595-2603.
(S24) W. Chen, X. Bao, Q. Zhu, D. Zhu, M. Qiu, M. Sun, R. Yang, *J. Mater. Chem. C*, 2015, **3**, 10070-10073.
(S25) M. M. Elnaggar, L. G. Gutsev, N. A. Emelianov, P. M. Kuznetsov, L. A. Frolova, S. M. Aldoshin, P. A. Troshin, *ACS Appl. Energy Mater.* 2022, **5**, 5388–5394.
(S26) Y. Kim, G. Kim, N. J. Jeon, C. Lim, J. Seo, B. J. Kim, *ACS Energy Lett.* 2020, **5**, 3304–3313.
(S27) Y. Kim, E. H. Jung, G. Kim, D. Kim, B. J. Kim, J. Seo, *Adv. Energy Mater*. 2018, **8**, 1801668.
(S28) L. Liang, N. Shibayama, H. Jiang, Z. Zhang, L. Meng, L. Zhang, Can Wang, N. Zhao, Y. Yu, S. Ito, J. Wu, J. Chen, P. Gao, *J. Mater. Chem. A*, 2022,**10**, 3409-3417.
(S29) Z. Yao, F. Zhang, Y. Guo, H. Wu, L. He, Z. Liu, B. Cai, Y. Guo, C. J. Brett, Y. Li, C. V. Srambickal, X. Yang, G. Chen, J. Widengren, D. Liu, J. M. Gardner, L. Kloo, L. Sun, *J. Am. Chem. Soc.* 2020, **142**, 17681–17692.
(S30) N. Y. Nia, F. Matteocci, L. Cina, A. D. Carlo, *ChemSusChem* 2017, **10**, 3854-3860.
(S31) D. Xu, Z. Gong, Y. Jiang, Y. Feng, Z. Wang, X. Gao, X. Lu, G. Zhou, J.-M. Liu, J. Gao, *Nat. Commun.* 2022, **13**, 7020
(S32) Y. Y. Kim, T.-Y. Yang, R. Suhonen, A. Kemppainen, K. Hwang, N. J.Jeon, J. Seo, *Nat. Commun*. 2020, **11**, 5146.
(S33) E.H. Jung, N.J. Jeon, E.Y. Park, C.S. Moon, T.J. Shin, T.-Y. Yang, J.H. Noh, J. Seo, *Nature*, 2019, **567**, 511-515.
(S34) J. You, F. Guo, S. Qiu, W. He, C. Wang, X. Liu, W. Xu, Y. Mai, , *J. Energy Chem*., 2019, **3**, 192-198.
(S35) S. Mu, Q. Ye, X. Zhang, S. Huang, J. You, *Front. Optoelectronics,* 2020, **13**, 265-271.
(S36) A. M. Elseman, M.S. Selim, L. Luo, C.Y. Xu, G. Wang, Y. Jiang, D.B. Liu, L.P. Liao, Z. Hao, Q. L. Song*, Chemsuschem,* 2019, **12**, 3808-3816.
(S37) M. Afzali, A. Mostafavi, T. Shamspur, *J. Alloys Compd.,* 2020, **817**, 152742.
(S38) D. Zou, F. Yang, Q. Zhuang, M. Zhu, Y. Chen, G. You, Z. Lin, H. Zhen, Q. Ling, *ChemSusChem,* 2019, **12**, 1155-1161.
(S39) Q. Hu, E. Rezaee, M. Li, Q. Chen, C. Li, S. Cai, H. Shan, Z.-X. Xu, *Sol. RRL,* 2020, **4**, 1900340.
(S40) D. Papadatos, D. Sygkridou, E. Stathatos, *Appl. Nanosci.*, 2020, **10**, 2165-2175.
(S41) J. Wang, Q. Hu, M. Li, H. Shan, Y. Feng, Z.-X. Xu, *Sol. RRL*, 2020, **4**, 2000109.
(S42) Z. Ye, J. Zhou, J. Hou, F. Deng, Y.-Z. Zheng, X. Tao, *Sol. RRL*, 2019, **3**, 1900109.
(S43) M. Alidaei, M. Izadifard, M.E. Ghazi, *Opt. Quant. Electron.,* 2020, **52**, 209.
(S44) Q. Hu, E. Rezaee, Q. Dong, H. Shan, Q. Chen, L. Wang, B. Liu, J.-H. Pan, Z.-X. Xu*, Sol. RRL*, 2019, **3**, 1800264.
(S45) S. Öz, A.K. Jena, A. Kulkarni, K. Mouri, T. Yokoyama, I. Takei, F. Ünlü, S. Mathur, T. Miyasaka, *ACS Energy Lett.,* 2020, **5**, 1292-1299.
(S46) H.-C. Hsieh, C.-Y. Hsiow, Y.-A. Su, Y.-C. Liu, W. Chen, W.-Y. Chiu, Y.-C. Shih, K.-F. Lin, L. Wang, *J. Power Sources,* 2019, **426**, 55-60.
(S47) I. Jeong, J.W. Jo, S. Bae, H.J. Son, M.J. Ko, *Dyes and Pigm.,* 2019, **164**, 1-6.
(S48) G. Wu, X. Dong, G. Cui, R Sun, X. Wu, M. Gu, Z. Zuo, Y. Liu, *Sol Energy.* 2022, **237**, 153-160.
(S49) N. Ishida, A. Wakamiya, A. Saeki, *ACS Photonics* 2016, **3**, 1678−1688.